magnetochemistry

MDPI

Article

Hydrogen Peroxide-Assisted Hydrothermal Synthesis of $BiFeO_3$ Microspheres and Their Dielectric Behavior

Asad Syed [1,*], Ashoka Siddaramanna [2], Abdallah M. Elgorban [1], D. A. Hakeem [3] and G. Nagaraju [4]

1 Department of Botany and Microbiology, College of Science, King Saud University, P.O. Box 2455, Riyadh 11451, Saudi Arabia; aelgorban@ksu.edu.sa
2 Department of Chemistry, School of Engineering, DayanandaSagar University, Bangalore 560 068, Karnataka, India; ashok022@gmail.com
3 School of Chemical Engineering and Light Industry, Guangzhou 510006, China; abdulhakeem.desh@gmail.com
4 Energy Materials Research Laboratory, Department of Chemistry, Siddaganga Institute of Technology, Tumkur 572103, India; nagarajugn@rediffmail.com
* Correspondence: assyed@ksu.edu.sa; Tel.: +966-011-4699611

Received: 5 August 2020; Accepted: 4 September 2020; Published: 9 September 2020

Abstract: Despite considerable efforts undertaken in a rapidly developing area of multiferroic research, synthesis of phase pure $BiFeO_3$ is still a matter of intensive research. In this work, we report the shape-controlled synthesis of pure $BiFeO_3$ microspheres via a facile hydrothermal route. The prepared $BiFeO_3$ powder has been characterized using powder X-ray Diffraction (XRD), Differential Thermal analysis (DTA), Scanning Electron microscopy (SEM), and impedance spectroscopy. Powder XRD analysis confirms the formation of pure rhombohedrally distorted perovskite with *R*3*c* space group. Scanning electron micrograph revealed that the prepared $BiFeO_3$ microspheres are nearly spherical in shape with uniform size distribution. The $BiFeO_3$ microspheres exhibit a dielectric constant value of ~110 at 1000 KHz, which is higher than the $BiFeO_3$ prepared by conventional solid-state reaction and sol–gel method. Variation of dielectric constant with temperature at different frequencies shows that the $BiFeO_3$ has a dielectric anomaly of ferroelectric to paraelectric type at 1093 K and this phenomenon is well supported by TGA results.

Keywords: hydrothermal synthesis; multiferroics; dielectric behavior; hydrogen peroxide; bismuth ferrite

1. Introduction

Nowadays, multiferroic (particularly $BiFeO_3$) materials are being widely investigated for spintronics, data-storage, sensors and multiple-state memory applications [1] because of their dual ordering (i.e., both magnetic and polar) characteristics at room temperature. $BiFeO_3$ crystallizes in a rhombohedral structure with *R3c* space group, and exhibits ferroelectric and antiferromagnetic properties at ~1100 and 630 K, respectively [2]. $BiFeO_3$ generates spontaneous polarization, ~100 $\mu C/cm^2$, from the lone pair of the Bi^{3+} ions, while the magnetic ordering originates from the superexchange interaction between the 3*d* electrons of the Fe^{3+} ions [3]. In recent years, $BiFeO_3$ has attracted significant interest owing to its high Curie temperature (1083 K) [4] and high Neel temperature (625 K) and its potential applications, such as water splitting, organic pollutants degradation (2.2 eV), solar cells and visible light optoelectronic devices [5–8]. However, $BiFeO_3$ finds limited application due to the high electric loss via leakage, existence of impurities, high electric coercive field, and weak magnetoelectric coupling due to the significant difference between the Curie temperature (1083 K) and the high Neel temperature (625 K), which leads to inadequate ferroelectric and magnetic properties in bulk $BiFeO_3$.

Different methods have been adopted in order to overcome the above limitations [2,3], including but not limited to different synthesis techniques, producing solid solution via rare earth ions doping at both Bi and Fe sites [2]. These methods can improve the stability, multiferroic features and magnetoelectric coupling effect of $BiFeO_3$. The magnetoelectric coupling effect can be effectively altered by tuning Curie temperature and Neel temperature. It was reported that the incorporation of rare earth ion at Bi site resulted in the modification of the ferroelectric properties, whereas the rare earth ion at the Fe site alters the magnetic properties [3]. The preparation of doped and un-doped $BiFeO_3$ via sol–gel and solid-state [1] reactions requires elevated temperature of 600–900 °C and complex/expensive reagents like citric acid and urea [9].

Therefore, there is an urgent need to develop new synthesis processes for obtaining pure $BiFeO_3$, which is a challenging task even today due to the appearance of secondary phases in $BiFeO_3$. It is very difficult to obtain single phase $BiFeO_3$ because of non-stoichiometric oxygen in the structure, which leads to the formation of undesirable impurity phases such as $BiFe_4O_9$, $Bi_{25}FeO_{39}$ and $Bi_{25}FeO_{40}$ [10]. The presence of $BiFe_4O_9$, $Bi_{25}FeO_{39}$ and $Bi_{25}FeO_{40}$ impurities significantly reduces the thermal stability of $BiFeO_3$, and they also increase the leakage current [11]. The synthesis of pure $BiFeO_3$ is quite subtle, because it is necessary to take both kinetic and thermodynamic properties into account. In this view, considerable effort has been made in the past for the controlled synthesis of $BiFeO_3$ owing to its size- and morphology-dependent magnetic, electrical, and optical properties [5,12–16]. However, the successive modulation of size and morphology of $BiFeO_3$ has yet to become a reality.

In the present paper, as the synthesis technique and reaction parameters play a crucial role in controlling the material properties, we successfully applied the hydrothermal synthesis route for the fabrication of single phase $BiFeO_3$ microspheres without any additional thermal treatment. The hydrothermal synthesis route possessed the potential to produce well-crystallized $BiFeO_3$ with controlled morphology and narrow distribution of particle size. The $BiFeO_3$ microspheres prepared by the hydrothermal method show higher dielectric constant value (~110 at 1000 KHz) than the $BiFeO_3$ prepared by conventional solid-state reaction (~20 at 100 KHz) and sol–gel method (~68 at 1M Hz). Additionally, $BiFeO_3$ has shown dielectric anomaly of ferroelectric to paraelectric type at 1093 K.

2. Experimental

2.1. Materials

The chemical reagents used in the work were bismuth nitrate ($Bi(NO_3)_3{\cdot}5H_2O$, 99%), Ferric nitrate ($Fe(NO_3)_3{\cdot}9H_2O$, 99%), Sodium hydroxide (NaOH, 90%), Potassium hydroxide (KOH, 90%), and Hydrogen peroxide (30% H_2O_2). All these analytical-grade purity chemicals were purchased from S D Fine-Chem Limited, India, and used without further purification.

2.2. Method

Amounts of 0.01 mol $Bi(NO_3)_3{\cdot}5H_2O$, 0.01 mol $Fe(NO_3)_3{\cdot}9H_2O$, 0.051 mol NaOH, 0.049 mol KOH were mixed with 12 mL acetone and stirred for 10 min. The reason for using high concentrations of NaOH and KOH was to sufficiently maintain the basic condition. During this, an exothermic reaction took place, and all the acetone evaporated. After thorough mixing, 4 mL H_2O_2 was added to provide an oxygen-enriched atmosphere to keep the Fe ion in Fe^{3+} form and convert hydroxide into oxide. The obtained resin-like suspension was poured into the Teflon-lined stainless-steel autoclave for hydrothermal treatment. The autoclave was sealed and maintained at 200 °C ± 5 for 24 h. After the completion of the reaction, the product was removed from the autoclave and washed with water and acetone several times and dried in a laboratory oven at 80 °C ± 5 for several hours.

2.3. Characterization

The structure and crystallinity of the prepared $BiFeO_3$ microspheres were characterized by PANalytical X'pert X-ray diffractometer (XRD) equipped with graphite monochromatized CuKa

radiation (Malvern Panalytical, Lelyweg, The Netherlands). Differential thermal analysis of $BiFeO_3$ microspheres was carried out from room temperature to 900 °C in pure oxygen atmosphere at a scan rate of 10 °C/min using Q600. Scanning electron microscope (SEM) images were taken with a JEOL. The SEM images were recorded by adding a small amount of sample onto the carbon conductive tape, and then gold was spurred for 9 s. Then, the gold-spurred samples were examined using SEM. The densities of the $BiFeO_3$ pellets (made with 2% polyvinyl alcohol as a binder) were measured using the Archimedes principle. The sintered $BiFeO_3$ ceramic specimens were polished and then electroded with high-quality silver paint on both sides of the disk-shaped samples. The dielectric and electrical properties of the samples were measured using a Hewlett Packard 4194A impedance gain phase analyzer (Commonwealth of Massachusetts, Woburn) over wide ranges of frequency 100 Hz–10 MHz and temperature room temperature to 830 °C.

3. Results and Discussion

The phase composition and structure of the as-prepared $BiFeO_3$ sintered at different temperatures were examined by powder XRD technique, and the observed XRD patterns are displayed in Figure 1. All the diffraction peaks in the XRD pattern of as-prepared $BiFeO_3$ (prepared at 200 °C/24 h by hydrothermal method) were consistent with the standard Joint Committee on Powder Diffraction Standards No. 86-1518 of pure $BiFeO_3$ having a rhombohedral crystal structure and *R*3*c* (161) space group. Additionally, the diffraction *(012)* peaks (2 theta = 22.34) of the as-prepared $BiFeO_3$ are intense and sharp, indicating the formation of well-crystallized single phase $BiFeO_3$. To investigate the effect of heat treatment on the $BiFeO_3$ samples, the powders were pressed into pellets and heat-treated at different temperatures (at 600, 700 and 800 °C), as shown in Figure 1. It is observed that the sintered $BiFeO_3$ pellets retain the rhombohedral structure with space group *R*3*c* at higher sintering temperature. The secondary phases associated with the $BiFeO_3$ such as $Bi_2Fe_4O_9$ and $Bi_{25}FeO_{40}$ are absent in the present study. This suggests the formation of crystalline single phase $BiFeO_3$ with good thermal stability. The crystallite size (D) of $BiFeO_3$ samples was calculated by following the Scherrer Formula.

$$D = (0.9\,\lambda)/(\beta\,\cos\theta) \quad (1)$$

where D is the crystallite size, λ is the wavelength of radiation, β is the full width at half maximum (FWHM) of the diffraction peak in radian and θ is Braggs angle. The crystallite sizes are calculated by considering the prominent diffraction peaks peaked at 2θ = 22.34 and 45.73, corresponding to the (*012*) and (*024*) planes, respectively. The average crystallite size of the as-prepared, 600, 700, and 800 °C samples was 34 ± 1.24, 41 ± 0.47, 43 ± 1.67, and 47 ± 0.94 nm, respectively.

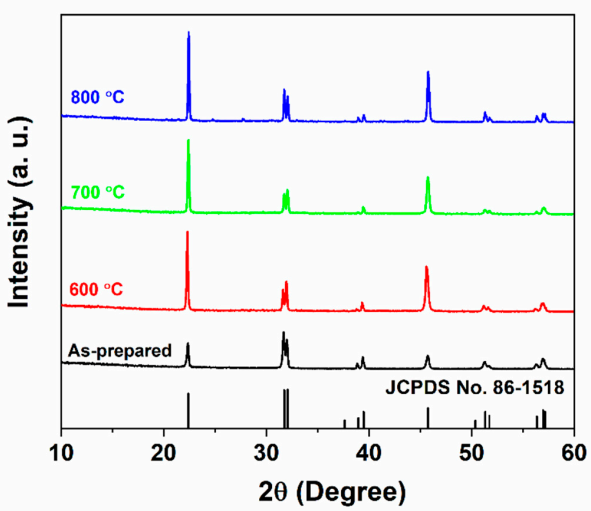

Figure 1. Powder XRD patterns of as-prepared $BiFeO_3$ microspheres and sintered at 600, 700, and 800 °C.

The formation of $BiFeO_3$ under the present experimental conditions can be explained as follows. Bismuth hydroxide and iron hydroxides were formed when bismuth nitrate and iron nitrate were mixed with sodium hydroxide and potassium hydroxide at room temperature (Equations (2) and (3)). Then, under hydrothermal conditions, the formed $Fe(OH)_3$ and $Bi(OH)_3$ undergo condensation to form $BiFeO_3$ microspheres (Equation (4)).

$$Bi^{3+}{}_{(aq)} + 3OH^{-}{}_{(aq)} \rightarrow Bi(OH)_3 \downarrow \quad (2)$$

$$Fe^{3+}{}_{(aq)} + 3OH^{-}{}_{(aq)} \rightarrow Fe(OH)_3 \downarrow \quad (3)$$

$$Bi(OH)_{3(s)} + Fe(OH)_{3(s)} \rightarrow BiFeO_3 \downarrow + 3H_2O_{(1)} \quad (4)$$

Figure 2 presents the DTA curve of the $BiFeO_3$ microspheres recorded between the temperatures 25 to 850 °C. The endothermic peak appearing at around 1088 K is attributed to the phase transformation ferroelectric to paraelectric, i.e., Curie temperature [17]. This observed Curie temperature is in agreement with the reported values for $BiFeO_3$ [18,19]. Furthermore, weak transition at 380 °C (653K) corresponds to antiferromagnetic phase transition.

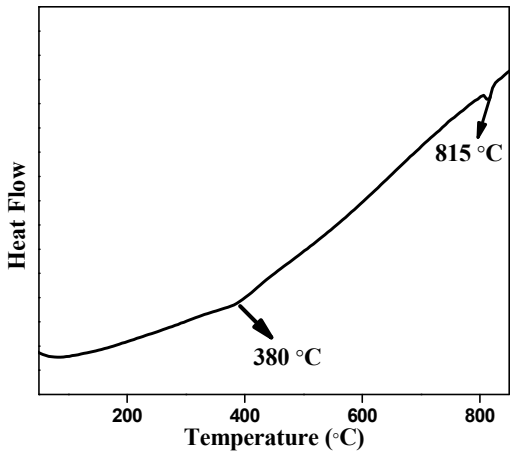

Figure 2. Dependence of heat flow with temperature for as-prepared $BiFeO_3$ microspheres.

To study the dielectric permittivity, the density of the $BiFeO_3$ was measured. The $BiFeO_3$ powders were pressed into a pellet of diameter 9 mm. The pressed $BiFeO_3$ pellets were submerged in water. The effective mass under water was determined by subtracting actual mass from the mass of the water displaced. Then, the volume of the $BiFeO_3$ pellets was determined. Finally, the mass was divided by the volume to estimate the average density [20]. The effect of temperature on the density of the pellets can be clearly seen in Figure 3. The density of the prepared $BiFeO_3$ pellets sintered at 500 °C, 600 °C, 750 °C and 800 °C was shown to be 81%, 85%, 83% and 94%, respectively. Therefore, with an increase in the sintering temperature, the density of the $BiFeO_3$ increases, with the maximum being found to be ~94% at 800 °C. The observed density is h when the sample is sintered at 800 °C. The observed density, ~94%, is close to the $BiFeO_3$ density (96%) reported by spark plasma sintering technique [21]. The lower density compared to the theoretical density may be due to the presence of little porosity in the pellets.

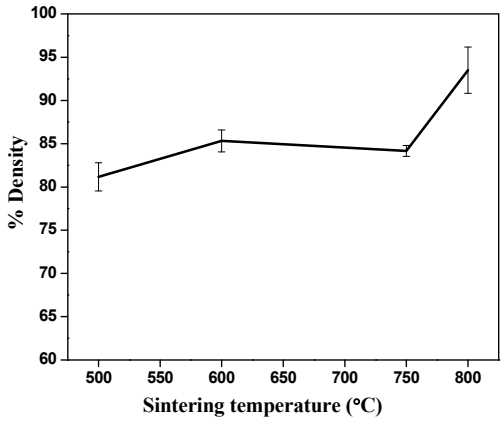

Figure 3. The variation of the density (%) of the $BiFeO_3$ against sintering temperature.

A typical scanning electron micrograph of the $BiFeO_3$ powder prepared by the present method is shown in Figure 4. It was observed that the $BiFeO_3$ powder exhibited a spherical structure with a rough surface. The average size of the $BiFeO_3$ spherical structures was found to be in the range of 20–30 µm. Each sphere is composed of significantly smaller agglomerated particles. The spherical structures are formed due to the high oxygen partial pressure [22]. The formation of high oxygen partial pressure is due to the decomposition of molten nitrate during heat treatment in a closed container according to Equation (5). Similar results were reported by Xiaobo He et al. for the synthesis of BiFeO3 in presence of potassium and sodium nitrate [23].

$$2NO_3{}^-{}_{(aq)} \rightarrow 2NO_{2(g)} + 1/2O_{2(g)} + O^{2-} \quad (5)$$

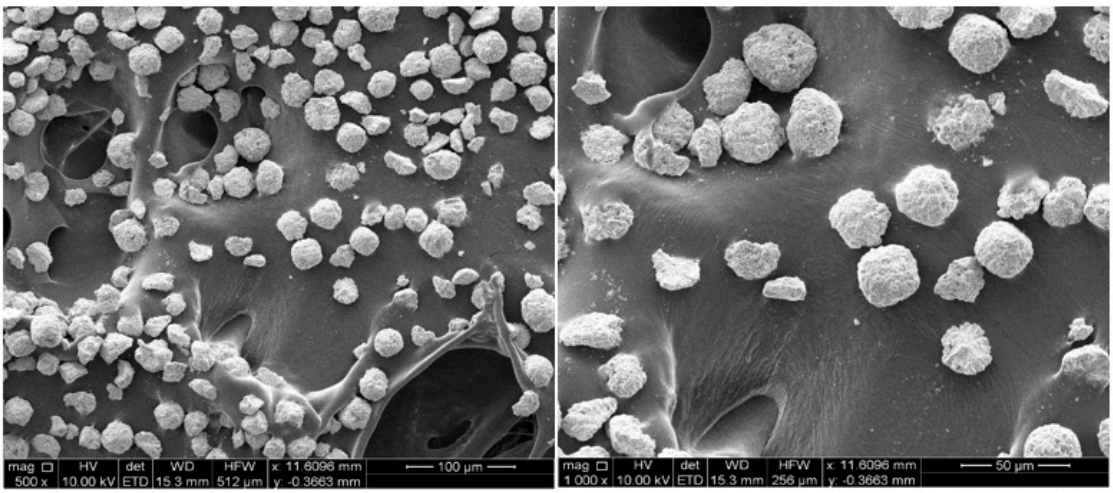

Figure 4. Scanning electron micrograph of the $BiFeO_3$ powder.

The mixture KOH and NaOH was used for precipitation in our synthesis with the aim to carry out the reaction similar to molten metal flux method. Generally, melts can be made more acidic (H_2O-rich) or basic (O^{2-} rich) by controlling the water content of the melt, based on the product formation requirement. In our synthesis, both iron nitrate and bismuth nitrate dissolves and heating at 200 °C in air-tight autoclave resulted in slow loss of water as vapors, thereby making the melt more basic and the product insoluble [24]. In addition, the excess added NaOH and KOH maintain a basic pH.

The effect of frequency on the dielectric constant and the dielectric loss factor of $BiFeO_3$ are presented in Figure 5. The dielectric constant is found to decrease slowly when frequency increases

from 100 Hz to 100 kHz, and then becomes almost constant, showing the usual dielectric dispersion [25]. It is observed from the figure that the prepared $BiFeO_3$ microsphere exhibit a high dielectric constant value of ~113 ± 4.64 at 1000 KHz, which is significantly higher than the hydrothermally derived Cr-substituted $BiFeO_3$ (50 at 0.2–1.2 MHz), and $BiFeO_3$ prepared by conventional solid-state (~20 at 100 KHz) and sol–gel reaction (~68 at 1M Hz) [25–27]. Generally, the dielectric properties of the relaxors depend on the microstructural characteristics such as grain size, grain-boundary character and pores. Therefore, microstructural control with an appropriate choice of additive can be critical in the applications. Better powder characteristics, such as a relatively uniform distribution of particle size and less particle agglomeration, obtained by the present method are believed to contribute to the resultant dielectric properties.

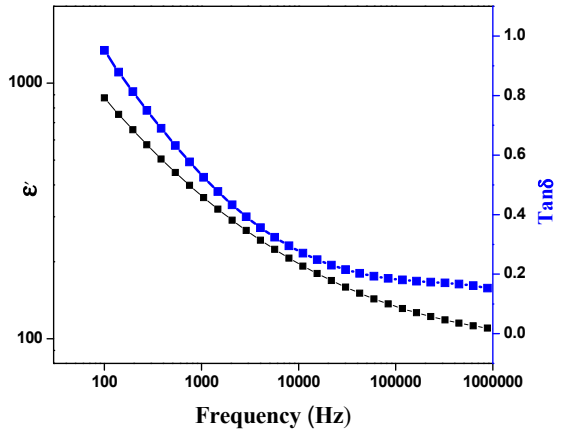

Figure 5. Variation of dielectric constant (ε) and dielectric loss ($\acute{\varepsilon}$) with frequency.

The effect of temperature on the dielectric constant is shown in Figure 6. The dielectric constant of the specimen was measured from room temperature to 850 °C at frequencies of 100, 500, 1000, and 10,000 kHz. It was found that the $BiFeO_3$ has a dielectric anomaly at 1093 K (the Curie temperature, Tc) suggesting the occurrence of ferroelectric–paraelectric phase transition.

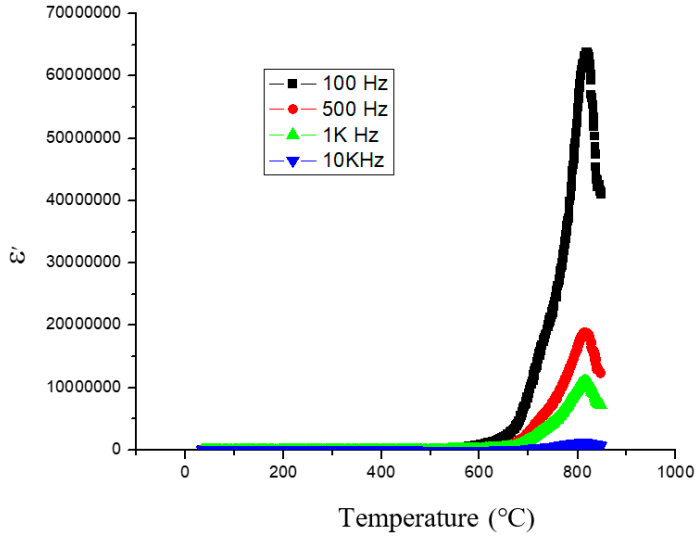

Figure 6. The effect of temperature on the dielectric constant of $BiFeO_3$.

4. Conclusions

$BiFeO_3$ microspheres were synthesized by direct precipitation followed by hydrothermal route from the mixture of iron nitrate and bismuth nitrate in the molten KOH/NaOH solution at temperature

as low as 200 °C. The prepared $BiFeO_3$ microspheres exhibit higher thermal stability up to 800 °C, and show larger dielectric constant values at different frequencies. The proposed method may be extended for the synthesis of other perovskite materials.

Author Contributions: Conceptualization, G.N. and A.S. (Asad Syed); methodology, A.S. (Ashoka Siddaramanna); software, A.S. (Ashoka Siddaramanna) and A.M.E.; formal analysis, A.S. (Ashoka Siddaramanna) and D.A.H.; investigation, A.S. (Ashoka Siddaramanna) and A.S. (Asad Syed); resources, G.N.; data curation, A.S. (Ashoka Siddaramanna), A.S. (Asad Syed) and G.N.; writing—original draft preparation, A.S. (Ashoka Siddaramanna), G.N.; writing—review and editing, A.S. (Ashoka Siddaramanna), A.S. (Asad Syed) and G.N.; supervision, A.S. (Asad Syed), and G.N.; project administration, G.N.; funding acquisition, A.M.E. All authors have read and agreed to the published version of the manuscript.

Funding: Researchers supporting project number (RSP-2020/56) King Saud University, Riyadh, Saudi Arabia.

Acknowledgments: The authors extend their appreciation to the researchers supporting project number (RSP-2020/56) King Saud University, Riyadh, Saudi Arabia.

Conflicts of Interest: The authors declare no conflict of interest.

References

1. Ma, Y.; Lv, P.; Duan, F.; Sheng, J.; Lu, S.; Zhu, H.; Du, M.; Chen, M. Direct Z-scheme $Bi_2S_3/BiFeO_3$ heterojunction nanofibers with enhanced photocatalytic activity. *J. Alloys Compd.* **2020**, *834*, 155158. [CrossRef]
2. Carvalho, T.T.; Manjunath, B.; Pérez de la Cruz, J.; Amaral, V.S.; Fernandes, J.R.A.; Almeida, A.; Moreira, J.A.; Vilarinho, R.; Tavares, P.B. Enhancement of resistivity and magnetization of $Bi_{1-x}La_xFe_{1-y}Mn_yO_3$ ceramics by composition optimization. *J. Alloys Compd.* **2020**, *835*, 155404. [CrossRef]
3. Liu, J.; Niu, M.; Wang, L.; Peng, C.; Xu, D. Effect of tuning A/B substitutions on multiferroic characteristics of $BiFeO_3$-based ternary system ceramics. *J. Mag. Mag. Mater.* **2020**, *510*, 166928–166937. [CrossRef]
4. Wang, J.; Neaton, J.B.; Zheng, H.; Nagarajan, V.; Ogale, S.B.; Liu, B.; Viehland, D.; Vaithyanathan, V.; Schlom, D.G.; Waghmare, U.V.; et al. Epitaxial $BiFeO_3$ Multiferroic Thin Film Heterostructures. *Science* **2003**, *299*, 1719–1722. [CrossRef] [PubMed]
5. Lou, J.; Maggard, P.A. Hydrothermal Synthesis and Photocatalytic Activities of $SrTiO_3$-Coated Fe_2O_3 and $BiFeO_3$. *Adv. Mater.* **2006**, *18*, 514–517.
6. Li, S.; Lin, Y.H.; Zhang, B.P.; Li, J.F.; Nan, C.W.J. $BiFeO_3/TiO_2$ core-shell structured nanocomposites as visible-active photocatalysts and their optical response mechanism. *Appl. Phys.* **2009**, *105*, 054310. [CrossRef]
7. Gao, F.; Yuan, Y.; Wang, K.F.; Chen, X.Y.; Chen, F.; Liu, J.M.; Ren, Z.F. Preparation and photoabsorption characterization of nanowires. *Appl. Phys. Lett.* **2006**, *89*, 102506. [CrossRef]
8. Joshi, U.A.; Jang, J.S.; Borse, P.H.; Lee, J.S. Microwave synthesis of single-crystalline perovskite $BiFeO_3$ nanocubes for photoelectrode and photocatalytic applications. *Appl, Phys. Lett.* **2008**, *92*, 242106. [CrossRef]
9. Tahir, M.; Riaz, S.; Khan, U.; Hussain, S.S.; Nairan, A.; Akbar, A.; Saleem, M.; Atiq, S.; Naseem, S. Enhanced structural and magnetic ordering in as-synthesized Ca doped bismuth iron oxide nanoceramics. *J. Alloys Compd.* **2020**, *832*, 154725. [CrossRef]
10. Auromun, K.; Choudhary, R.N.P. Structural, Dielectric and Electrical investigation of Zirconium and Tin modified 0.5BFO-0.5BST. *Mater. Chem. Phys.* **2020**, *250*, 123033. [CrossRef]
11. Selbach, M.; Einarsrud, M.-A.; Grande, T. On the Thermodynamic Stability of $BiFeO_3$. *Chem. Mater.* **2009**, *21*, 169–173. [CrossRef]
12. Achenbach, G.D.; James, W.J.; Gerson, R. Preparation of Single-Phase Polycrystalline $BiFeO_3$. *J. Am. Ceram. Soc.* **1967**, *50*, 437. [CrossRef]
13. Valant, M.; Axelsson, A.K.; Alford, N. Peculiarities of a Solid-State Synthesis of Multiferroic Polycrystalline $BiFeO_3$. *Chem. Mater.* **2007**, *19*, 5431–5436. [CrossRef]
14. Shetty, S.; Palkar, V.R.; Pinto, R. Size effect study in magnetoelectric $BiFeO_3$ system. *J. Phys.* **2002**, *58*, 1027–1030. [CrossRef]
15. Kim, J.K.; Kim, S.S.; Kim, W.J. Sol–Gel synthesis and properties of multiferroic $BiFeO_3$. *Mater. Lett.* **2005**, *59*, 4006–4009. [CrossRef]
16. Chen, C.; Cheng, J.; Yu, S.; Che, L.; Meng, Z. Hydrothermal synthesis of perovskite bismuth ferrite crystallites. *J. Cryst. Growth* **2006**, *291*, 135–139. [CrossRef]

17. Tabares-Munoz, C.; Rivera, J.P.; Monnier, A.; Schmid, H. Measurement of the quadratic magnetoelectric effect on single crystalline $BiFeO_3$. *J. Appl. Phys. Suppl.* **1985**, *24*, 1051–1053. [CrossRef]
18. Palkar, V.R.; John, J.; Pinto, R. Observation of saturated polarization and dielectric anomaly in magnetoelectric thin films. *Appl. Phys. Lett.* **2002**, *80*, 1628–1631. [CrossRef]
19. Iakovlev, S.; Solterbeck, C.H.; Kuhnke, M.; Es-Souni, M. Multiferroic thin films processed via chemical solution deposition: Structural and electrical characterization. *J. Appl. Phys.* **2005**, *97*, 094901. [CrossRef]
20. Fabienne, R.; Michael, T.; Thorsten, B.; Hans, H.; Peter, D.J.; Josef, R.; Juan, C.; Miguel, F. Particle density determination of pellets and briquettes. *Biomass Bioenergy* **2006**, *30*, 954–963.
21. Mazumder, R.; Chakravarty, D.; Bhattacharya, D.; Sen, A. Spark plasma sintering of $BiFeO_3$. *Mater. Res. Bull.* **2009**, *44*, 555–559. [CrossRef]
22. Fang, T.T.; Ting, C.C.; Miao, J.H. A Template-Free Synthesis of the One-Dimensional Nanostructure of Multiferroic $BiFeO_3$. *J. Am. Ceram. Soc.* **2009**, *92*, 3065–3069. [CrossRef]
23. Xiaobo, H.; Lian, G. Synthesis of pure phase $BiFeO_3$ powders in molten alkali metal nitrates. *Ceram. Int.* **2009**, *35*, 975–978.
24. Bondioli, F.; Bonamartini, C.A.; Leonelli, C.; Manfredini, T. Nanosized CeO_2 powders obtained by flux method. *Mater. Res. Bull.* **1999**, *34*, 2159–2166. [CrossRef]
25. Du, Y.; Cheng, Z.X.; Dou, S.X.; Shahbazi, M.; Wang, X.L. Enhancement of magnetization and dielectric properties of chromium-doped $BiFeO_3$ with tunable morphologies. *Thin Solid Film.* **2010**, *518*, e5–e8. [CrossRef]
26. Chang, F.; Zhang, N.; Yang, F.; Wang, S.; Song, G. Effect of Cr substitution on the structure and electrical properties of $BiFeO_3$ ceramics. *J. Phys. D* **2007**, *40*, 7799–7803. [CrossRef]
27. Liu, H.; Liu, Z.; Liu, Q.; Yao, K. Ferroelectric properties of $BiFeO_3$ films grown by sol–gel process. *Thin Solid Films* **2006**, *500*, 105–109. [CrossRef]